

RESEARCH ARTICLE | MAY 01 2007

Total dissociative electron attachment cross sections of selected amino acids

A. M. Scheer; P. Mozejko; G. A. Gallup; P. D. Burrow



J. Chem. Phys. 126, 174301 (2007)

<https://doi.org/10.1063/1.2727460>



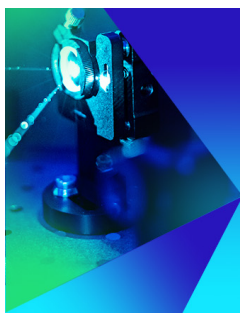
View
Online



Export
Citation

CrossMark

This article may be downloaded for personal use only. Any other use requires prior permission of the author and AIP Publishing. This article appeared in (citation of published article) and may be found at <https://doi.org/10.1063/1.2727460>



The Journal of Chemical Physics
Special Topic: Time-resolved
Vibrational Spectroscopy

Submit Today



Total dissociative electron attachment cross sections of selected amino acids

A. M. Scheer

Department of Physics and Astronomy, University of Nebraska-Lincoln, Lincoln, Nebraska 68588-0111

P. Mozejko

Atomic Physics Division, Faculty of Applied Physics and Mathematics, Gdansk University of Technology, 870-952 Gdansk, Poland

G. A. Gallup and P. D. Burrow^{a)}

Department of Physics and Astronomy, University of Nebraska-Lincoln, Lincoln, Nebraska 68588-0111

(Received 20 February 2007; accepted 19 March 2007; published online 1 May 2007)

Total dissociative electron attachment cross sections are presented for the amino acids, glycine, alanine, proline, phenylalanine, and tryptophan, at energies below the first ionization energy. Cross section magnitudes were determined by observation of positive ion production and normalization to ionization cross sections calculated using the binary-encounter-Bethe method. The prominent 1.2 eV feature in the cross sections of the amino acids and the closely related HCOOH molecule is widely attributed to the attachment into the $-\text{COOH } \pi^*$ orbital. The authors discuss evidence that direct attachment to the lowest σ^* orbital may instead be responsible. A close correlation between the energies of the core-excited anion states of glycine, alanine, and proline and the ionization energies of the neutral molecules is found. A prominent feature in the total dissociative electron attachment cross section of these compounds is absent in previous studies using mass analysis, suggesting that the missing fragment is energetic H^- . © 2007 American Institute of Physics. [DOI: 10.1063/1.2727460]

I. INTRODUCTION

Bond breaking through the formation and dissociative decay of temporary anion states, the dissociative electron attachment (DEA) process, is likely to be the dominant means by which biomolecules are degraded by free electrons with energies below the ionization threshold. Because of the challenges in measuring gas phase densities of low volatility molecules, absolute cross sections for compounds such as the amino acids are difficult to obtain. However, an alternative approach exploited recently¹ for three DNA bases and surrogate compounds for the other components of a DNA nucleotide yields cross section magnitudes within reasonable error limits. In this method, the total anion current produced in a collision cell is acquired as a function of electron energy and compared to the total cation current at the peak of the ionization cross section. The cross section for the latter process is obtained by semiempirical means using the binary-encounter-Bethe² (BEB) or Deutsch-Märk³ (DM) approach and used to place the anion currents on an absolute cross section scale. According to Feil *et al.*,⁴ comparisons between DM calculated ionization cross sections and experimental measurements show agreement between 5% and 20% for a variety of molecules.

In the present work, DEA cross sections for glycine, alanine, phenylalanine, proline, and tryptophan are reported. The ionization cross sections used for normalization were

computed by Mozejko using the BEB scheme and are also provided. In addition, we address the characteristics of the resonance responsible for the lowest lying peak in the DEA cross sections of these compounds and those in the region of the core-excited anion states.

II. BEB CALCULATIONS

Theoretical and computational procedures in the present work are essentially the same as those in a previous BEB study of ionization in selected components of DNA and RNA.⁵ The binary-encounter-Bethe model,^{6,7} which is a simplified version of the binary-encounter-dipole model,⁶ is based on a combination of two theories by Mott⁸ and by Bethe.⁹ The method has been successfully employed for calculation of total electron-impact ionization cross sections of a variety of molecules, e.g., Refs. 10 and 11. In this approximation the electron-impact ionization cross section per molecular orbital is given by the relation

$$\sigma^{\text{BEB}} = \frac{S}{t+u+1} \left[\frac{\ln t}{2} \left(1 - \frac{1}{t^2} \right) + 1 - \frac{1}{t} - \frac{\ln t}{t+1} \right],$$

where $S = 4\pi a_0^2 N R^2 / B^2$ ($a_0 = 0.5292 \text{ \AA}$, $R = 13.61 \text{ eV}$), $u = U/B$, $t = T/B$, and T is the energy of the impinging electron. All molecular parameters necessary to compute the ionization cross section within the BEB approach, i.e., the electron binding energy B , the kinetic energy of the orbital U , and the orbital occupation number, were obtained for the ground states of the geometrically optimized molecules with the Hartree-Fock method using the GAUSSIAN 03 code¹² and the

^{a)} Author to whom correspondence should be addressed. Electronic mail: pburrow1@unl.edu

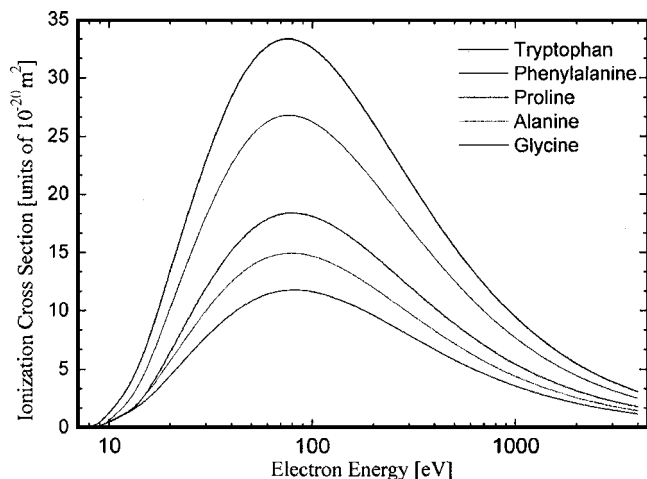


FIG. 1. BEB single ionization cross sections (in order of decreasing magnitude) for tryptophan, phenylalanine, proline, alanine, and glycine.

Gaussian 6-311G basis set. Because the valence orbital energies obtained this way usually have slightly higher values than the experimental ones, we additionally performed outer valence Green's function calculations of correlated electron affinities and ionization potentials,¹³ also with the GAUSSIAN 03 code. The total cross section for single electron-impact ionization at energies ranging from the ionization threshold up to 4000 eV has been obtained as the sum of σ^{BEB} for all occupied molecular orbitals. The calculated single ionization cross sections of the five amino acids are shown in Fig. 1.

III. EXPERIMENT

The reader is referred to Aflatooni *et al.*¹ for the details of our apparatus. Briefly, a magnetically collimated electron transmission spectrometer¹⁴ used previously to determine the vertical attachment energies (VAEs) of these amino acids¹⁵ was modified to include guard plates allowing small currents to be measured on a cylindrical electrode, coaxial with the electron beam, in the collision cell. An oven containing the sample powder is attached directly to the collision cell. The oven and cell temperatures are independently controlled, with the cell maintained about 10 °C warmer. The approximate sample oven temperatures employed were 139 °C (glycine), 129 °C (alanine), 118 °C (proline), 134 °C (phenylalanine), and 179 °C (tryptophan).

Electron beam currents in the range of 50–80 nA were used with resolutions of 100–150 meV. The energy scale was calibrated with reference to the 2.25 eV DEA peak observed by addition of N₂O to the cell. The apparatus was tested in N₂O by measuring the ratio of anion current at the 2.25 eV DEA peak to the cation current at the maximum in the positive ionization cross section. This ratio was within 10% of that given by the known cross sections for the two processes. Because of the sensitivity of anion currents to the potentials on the entrance and exit electrodes of the collision cell and the difficulty in maintaining these regions electric field free, we estimate errors in the ratio measurements to be within $\pm 50\%$ below 4 eV and $\pm 25\%$ above 4 eV.

No corrections have been applied to compensate for the variations in effective scattering path length with electron

energy that arise from small transverse velocity components of the electron beam entering the collision chamber. The resultant helical motion enhances the apparent magnitude of the low energy DEA peaks relative to those at higher energy. Estimates of the magnitude of this effect suggest that it falls well within the error limits cited here, as do our test measurements in N₂O. Nevertheless, it is useful to point out that this effect could be quite significant for DEA peaks occurring near zero energy and that it may depend on tuning of the trochoidal monochromator.

IV. RESULTS

In Fig. 2 we present the DEA cross sections for the selected amino acids. The sharp downturns in anion currents at the upper ends of the scans are produced by the onset of positive ionization. For convenience in our later discussion, a short vertical line indicates the energy for electron attachment into the empty π^* orbital associated with the –COOH group in each compound as determined from a previous electron transmission spectroscopy (ETS) study.¹⁵ For reference, these VAEs are as follows: 1.93 eV (glycine), 1.80 eV (alanine), 1.91 eV (proline), 1.85 eV (phenylalanine), and 1.60 eV (tryptophan). Our results are summarized in Table I which lists the maximum positive ionization cross sections as calculated with the BEB method, the energies of the peaks in the negative ion yields, the cation/anion ratio at these peaks, and the resulting DEA cross sections.

V. DISCUSSION

For purposes of our discussion, the DEA spectra shown in Fig. 2 can be divided into the region below 4 eV, in which one expects shape resonances to dominate electron scattering, and above 4 eV, where core-excited resonances associated with the virtual excitation of electronically excited states will be present. It should be noted that there is no clear separation between these regions, and that higher lying shape resonances may well contain significant admixtures of core-excited states.

A. Shape resonances

1. Amino acids

In the shape resonance regime, resonances have been explored previously¹⁵ using ETS, and the assignments supported with molecular orbital calculations. A common feature in the total scattering cross section is the π^* resonance residing primarily on the –COOH group. The VAEs, for formation of this resonance, range from 1.6 to 1.93 eV as listed above. The ET spectrum of formic acid HCOOH displays a similar resonance at 1.73 eV,¹⁵ and an earlier transmission study with higher energy resolution¹⁶ showed evidence for vibrational motion of this temporary anion state. The unsaturated side groups in phenylalanine and tryptophan also produce strong π^* resonances in the ET spectrum at other energies, but these will play no role in this discussion.

The common feature in the DEA cross sections we observe between 1.18 and 1.27 eV has been seen previously in mass analyzed data in glycine,^{17–19} alanine,²⁰ proline,²¹ and tryptophan.²² A similar feature appears in HCOOH.^{23–27} In

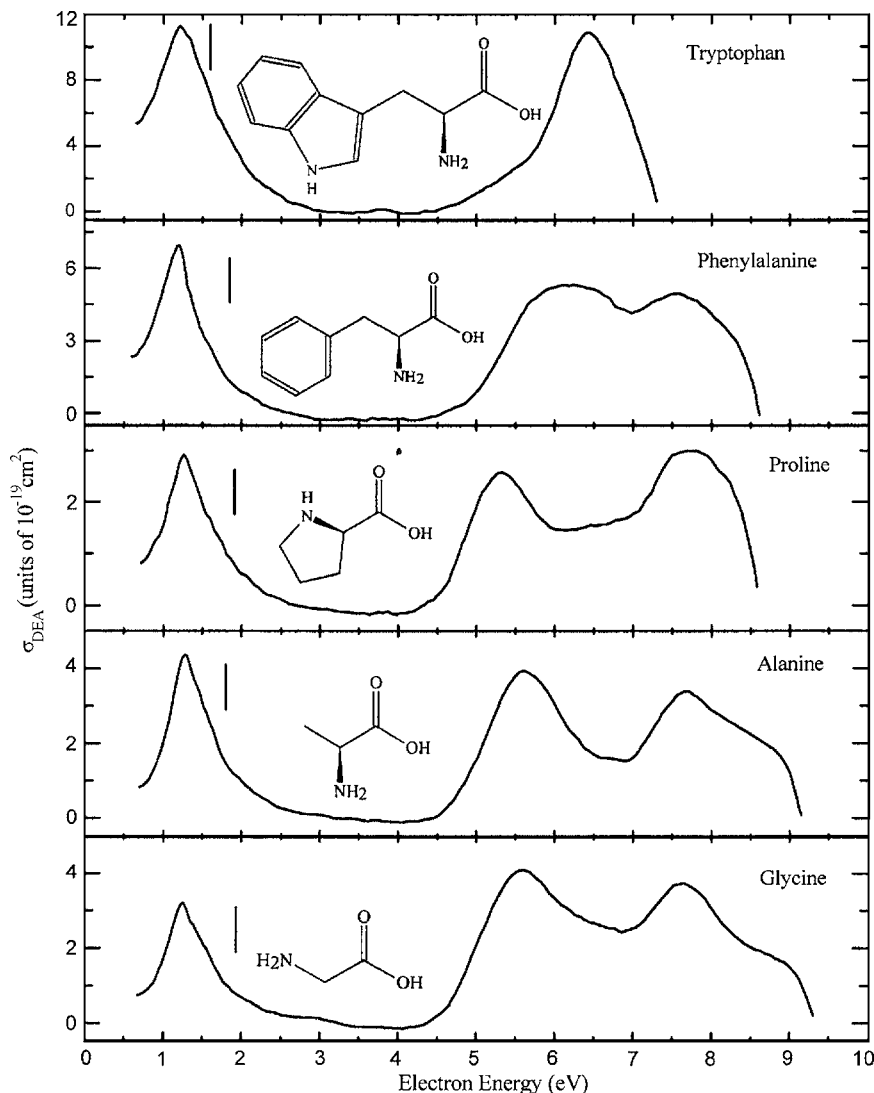


FIG. 2. Total dissociative electron attachment cross sections of glycine, alanine, proline, phenylalanine, and tryptophan. The vertical lines indicate the vertical attachment energies into the π^* orbital of the $-\text{COOH}$ group. The sharp decreases in anion current at high energies reflect the onset of positive ionization.

each case, mass analysis indicates that the fragment is $[\text{M}-\text{H}]^-$, the parent molecular anion minus a H atom. The measurements with high energy resolution suggest that this feature displays a near vertical onset, indicating that the threshold for this DEA process lies just below the peak energy. Bond energy and electron affinity considerations are consistent with this conclusion and indicate as well that H atom loss in HCOOH occurs from the $-\text{COOH}$ group.

Because of the proximity of the 1.2 eV DEA peaks to the $-\text{COOH}$ π^* resonances determined by ETS, all of the experimental papers cited above that report an assignment for the amino acids or for HCOOH attribute these DEA peaks to the initial electron occupation of the normally empty π^* orbital on this moiety. This assignment was also supported recently in calculations on HCOOH by Rescigno *et al.*,²⁸ showing that out-of-plane distortions could indeed couple the initial π^* resonance to the σ^* resonance that leads to the $\text{H} + \text{HCOO}^-$ product. However, this work did not show that the distorted geometries were actually induced by occupation of the π^* orbital and reached by the initially planar anion state. In particular, the out-of-plane distortion was primarily forced on the H atom connected to the C atom. Consequently, while these calculations show that π^*/σ^* coupling is a possible

route to DEA, they do not prove that it is the actual mechanism responsible.

None of the published DEA data, nor our own given in Fig. 2, shows evidence for a peak in the production of the $[\text{M}-\text{H}]^-$ fragment at the actual π^* resonance energy given by the VAE. Rather, the peaks occur 0.4–0.7 eV lower. This behavior is in sharp contrast to results in thymine, cytosine, and adenine,¹ in which peaks in production of $[\text{M}-\text{H}]^-$ occur within experimental error at the energies of the π^* VAEs. The mechanism in this case was attributed to initial attachment to the π^* orbital followed by distortions that couple π^* to an antibonding $\sigma^*(\text{N}-\text{H})$ orbital. In the amino acids the DEA cross section is limited on the low energy side by the thermodynamic threshold for the process, and thus the peak value of the cross section could occur even lower. Such shifts between the peak in the capture cross section, occurring at the VAE, and the DEA peak are well known but generally are observed in shorter lived $^2\Sigma$ anion states²⁹ rather than to the anions derived from initial occupation of π^* orbitals.

2. HCOOH

Because of the significance of HCOOH in modeling the behavior of the amino acids, we take a closer look here at its

TABLE I. Peak ionization cross sections computed by the binary-encounter-Bethe (BEB) procedure, cation/anion ratios for selected features, and the normalized total DEA cross sections.

	BEB peak cation cross section (units of 10^{-16} cm 2)	Electron energy (eV)	Cation/anion ratio	DEA cross section (units of 10^{-19} cm 2)
Glycine	11.80	1.25	3000	3.9
		5.55	2400	4.9
		7.60	2600	4.5
Alanine	14.90	1.27	3400	4.4
		5.60	3900	3.8
		7.63	4800	3.1
Proline	18.43	1.25	6300	2.9
		5.31	6100	3.0
		7.70	5100	3.6
Phenylalanine	26.83	1.18	3900	6.9
		6.45	5000	5.4
		~7.7	6300	4.3
Tryptophan	33.33	1.21	3000	11.1
		6.44	3400	9.8

anion states. In Fig. 3 we illustrate the two lowest virtual orbitals of the planar HCOOH molecule. These were determined from *ab initio* HF calculations using the 6-31G(*d*) basis set for both geometry optimization and electronic structure.³⁰ The π^* orbital has substantial amplitude on both the oxygen atoms bonded to carbon, not just that in the double bond. The signs of the wave functions indicate a force pushing the oxygens toward each other and away from the carbon atom upon occupation of the orbital, and thus, motion of the anion in the O–C–O bending vibration is expected, as assigned to sharp structure appearing in the total scattering cross section reported in Ref. 16.

The lowest σ^* orbital is located primarily on the OH bond. Occupation of this orbital by the incident electron stretches the OH bond, thus decreasing the orbital energy. The DEA product H+HCOO $^-$ is clearly permitted by symmetry in the planar geometry through the $^2\Sigma$ resonance associated with occupation of this σ^* orbital. This pathway to dissociation in HCOOH appears not to have been considered previously and could contribute to the DEA cross section without the necessity of nonplanar distortions, allowing coupling to the π^* resonance.

Unfortunately, and in contrast to resonances associated with occupation of π^* orbitals, low-lying σ^* resonances in molecules containing second row elements are not apparent in total scattering cross sections as viewed by ETS, either because of their short lifetimes or because they are obscured by strong π^* resonances. The virtual orbital energies (VOEs) of the two orbitals shown in Fig. 3 are 5.1076 (π^*) and 6.0491 (σ^*), in eV. Numerous studies³¹ have shown that π^* VOEs determined with appropriate basis sets are well correlated with measured VAEs in unsaturated compounds. Using the empirical scaling described in Ref. 32, the π^* resonance of HCOOH is predicted to lie at 1.88 eV, in very good agreement with experiment. Scaling is problematic for the σ^* resonances because of the absence of ETS values with which to form a correlation. Using the same π^* scaling,³² the σ^* resonance is predicted to lie at 2.59 eV. The σ^* resonance would

lie at 2.90 eV, with the scaling used previously for the C–Cl σ^* orbitals in chloroalkanes,³³ resonances that are visible in the total scattering cross section. Neither of these estimates is justifiable in detail, but together they may provide a rough estimate for the location of this anion state.

In an attempt to characterize the $^2\Pi$ and $^2\Sigma$ anion states of HCOOH more rigorously, Gallup³⁴ has carried out preliminary calculations of their energies and lifetimes using the discrete model finite element method³⁵ (DMFEM) with a modification suggested by Hazi.^{36,37} As computed with a 6-31G(*d*) basis set in the equilibrium geometry of the neutral molecule, the $^2\Pi$ anion state energy was determined to be 2.42 eV, 0.68 eV above the experimental value. The width Γ of the resonance was 0.81 eV. An experimental upper bound for the width may be obtained from the ETS (Ref. 15) measurements. Assuming a Lorentzian profile for this resonance, as viewed in the total scattering cross section, a width of 1.36 eV is obtained which represents the combined effect of the finite lifetime and Franck-Condon factors for the attachment process. The DMFEM calculations thus give results

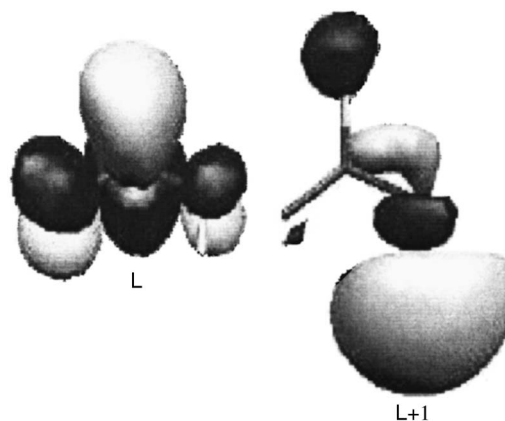


FIG. 3. The lowest unoccupied molecular orbital (LUMO) and LUMO+1 virtual orbitals of HCOOH from *ab initio* HF calculations using the 6-31G(*d*) basis for geometry optimization and electronic structure.

which are in general accord with the experimental data for the $^2\Pi$ anion state, although there is room for further improvement. Enlarging the basis set is expected to lower the calculated energy and to increase the calculated width.

The DMFEM calculated properties of the $^2\Sigma$ resonance are dramatically different from that of the $^2\Pi$ resonance discussed above. The resonance energy is computed to lie at 5.28 eV, but its width is found to be 5.79 eV. Such a large Γ makes it clear why this feature is not observed in the total scattering cross section. On the other hand, on each side of the nominal resonance energy, the calculated width decreases, and in the low energy wing of the resonance the width reaches approximately 3 eV at an electron energy corresponding to the maximum in the DEA cross section. It would thus seem possible that such a resonance could participate in DEA to produce $[M-H]^-$, and one would expect that the peaks would be shifted to substantially lower energies owing to the short resonance lifetime.

Finally, a recent study³⁸ of vibrational excitation in HCOOH with high energy resolution provides additional support for the role of the σ^* orbital. The cross section for excitation of the OH stretching mode declines slowly from its peak value near threshold, in contrast to the behavior of other vibrational modes that display peaks at the π^* VAEs in addition to a threshold peak. As pointed out by Allan,³⁸ the OH stretching mode appears to be excited through a mechanism other than the π^* resonance, and he suggests that it could be related to a broad OH σ^* shape resonance. He notes as well the presence of cusp like features in the OH stretching mode excitation functions for $\nu=1$ and 2 lying at the thresholds for higher levels of this mode. Most relevant to the present work, he points out a dip in the DEA cross section data of Pelc *et al.*²⁵ at the energy for excitation of four quanta of the OH stretch. From the measurements of Allan³⁸ in HCOOH, the differential cross section for excitation of the $\nu=3$ OH level, barely discernible in his data, may be estimated. Assuming that the process is isotropic, the total cross section near 2 eV is approximately 1.3×10^{-18} cm². It is interesting to note that the DEA cross sections, discussed below, are comparable or smaller in magnitude than this value. Excitation to this level, which lies energetically near the threshold for the DEA process, shows that the time dependent resonance wave function still has sufficient amplitude to excite the $\nu=3$ level of the neutral molecule and produce the measured cross section. The DEA cross section would be expected to be smaller, and this is also consistent with a common resonance source for both processes. These results, in total, provide a consistent case for a common origin for both the OH vibrational excitation and the DEA process leading to $HCOO^-+H$. The same scenario would apply to the low energy DEA peaks in the amino acids presented here.

3. DEA cross section magnitudes

Two measurements of the absolute DEA cross section of the 1.2 eV peak in HCOOH have been carried out. Pelc and co-workers^{24,25} report a peak value of $(1.7 \pm 0.6) \times 10^{-18}$ cm², while Prabhudesai *et al.*²⁶ find 1.4×10^{-18} cm². These values are roughly 50% larger than that of tryptophan and a factor of 5 larger than that of proline, the

smallest cross section of the amino acids studied. However, Martin *et al.*²⁷ argue that the electron attachment cross section to clusters of HCOOH is at least three orders of magnitude larger than to the monomer. If this applies to the DEA cross section near 1.2 eV, then the presence of even slight amounts of the dimer could cause the cross section to appear larger. Thus the numbers cited above may be upper bounds, and the cross section for HCOOH may lie closer to those observed in the amino acids.

Of the amino acids, tryptophan has the largest DEA cross section near 1.2 eV and proline has the smallest. The oven source temperatures for these compounds are also the highest and lowest, respectively, and thus it should be noted that thermally excited vibrational levels may play a role in the relative cross sections.

Finally, we note that estimates of the total DEA cross sections at the 1.2 eV feature have been given elsewhere for glycine^{18,19} (5×10^{-16} and $\sim 10^{-16}$ cm²) and for alanine (1.5×10^{-16} cm²).²⁰ The reasons for these substantial overestimates have been discussed previously.¹

4. Sharp structures

We end our discussion of shape resonances with a few comments relevant to the amino acids and additional sharp structure that may appear in the DEA cross sections. At the temperatures generally employed in gas phase studies, conformers of the amino acids that have substantial dipole moments may be present. The best studied of these is glycine, in which a dipole bound anion state has been observed by Johnson *et al.*³⁹ that is attributed to a conformer of the neutral with a dipole moment in excess of 5 D, easily capable of binding an electron by the 95 meV, measured by Johnson *et al.*³⁹ According to the calculations of Simons *et al.*,⁴⁰ the excited conformer lies approximately 35 meV above the lowest lying conformer.

Coupling of the dipole bound $^2\Sigma$ anion state to the lowest valence anion state of this symmetry, which is likely to be that associated with the OH bond as in HCOOH, may lead to the presence of vibrational Feshbach resonances⁴¹ in the DEA yield. Such a mechanism has been invoked to explain the presence of sharp peaks in the $[M-H]^-$ DEA cross sections of the DNA bases as well as structures in the total scattering cross sections of halo-substituted bases.⁴² The most extensive treatment is found in Ref. 43. Candidates for these features may include the 1.57 eV peak and the smaller 1.88 eV feature deconvoluted from the DEA spectrum in glycine¹⁹ and the 1.42 eV peak in alanine.²⁰ The first of these in each compound is generally consistent with the approximate location of the $\nu=4$ OH stretching level of the dipole bound anion state (assuming a dipole binding energy of approximately 0.1 eV), keeping in mind the rather strong anharmonicity resulting from the avoided crossing of the valence and dipole bound anion states as the OH bond is lengthened.⁴³ These signals would only arise from the amino acid conformations present in the gas beam that have supercritical dipole moments.

B. Core-excited resonances

We focus first on the two most prominent peaks above 4 eV in the DEA spectrum of glycine, alanine, and proline appearing in Fig. 2. The lower of these, lying at 5.55 and 5.60 eV in glycine and alanine, respectively, and at 5.31 eV in proline, are in good agreement with the peak energies for the major fragment anions observed in the mass selected studies of Refs. 18–22. In alanine,²⁰ for example, the average peak energy of the two dominant fragments reported, COOH^- and OH^- , is 5.56 eV compared to our peak energy in the total cross section of 5.60 eV. These fragments are the largest *reported* contributors to this peak in all three of these amino acids.

Summing the contributions from all anion fragments to the alanine peak near 5.6 eV in the data of Ptasińska *et al.*,²⁰ we find a total that is 0.3 of that for production of $(\text{A-H})^-$ at 1.27 eV. In contrast, the total cross section in Fig. 2 shows that these features almost have the same size. Even bearing in mind the rather large error limits of the present data, this suggests that there is some kinetic energy discrimination in the collection of the mass analyzed fragments. This is not surprising considering the weak fields used to draw the anions toward the mass analyzer, and the problem may be most serious in the case of H^- . A similar summation in glycine¹⁹ yields a fragment total that is 0.45 of $(\text{G-H})^-$. In proline,²¹ the sum is only 0.05 of that for $(\text{Pro-H})^-$. A very recent study⁴⁴ of anion production in several amino acids and their methyl esters has been carried out using time of flight techniques for mass analysis. In principle this approach should be less susceptible to kinetic energy discrimination because of the pulsed injection of the ions. For reasons not specified, the apparatus was not capable of observing H^- . The sum of all other anion fragments was given as a function of electron energy, and in glycine the $[\text{G-H}]^-$ peak was found to be about six times larger than the summed contribution at 5.6 eV. This result is consistent with H^- being the major ion component released at this energy.

This effect is even more dramatic in the peak near 7.6 eV in the total DEA cross section which appears to be completely absent in the mass analyzed data for glycine and alanine. In proline this peak appears in the yield of COOH^- and OH^- , but these sum to only 0.04 of the cross section for $(\text{Pro-H})^-$. These results imply again that this peak in the total DEA cross section consists primarily of rather energetic H^- .

The orbital assignments of the core-excited temporary anion states have not been determined, to our knowledge. One possible sequence of core-excited resonances in glycine, alanine, and proline could arise from the promotion of a bound electron of the neutral molecule out of each of the occupied molecular orbitals into a low lying normally empty orbital, joined by an additional electron in either the same or a higher lying empty orbital. If the outer two electrons remain in the same configuration in each anion state, trends in the core-excited state (CES) energies might be expected to reflect the relative energies of the occupied orbitals.

We test this conjecture in glycine by noting that the separation between the 5.55 and 7.60 eV DEA peaks in Fig.

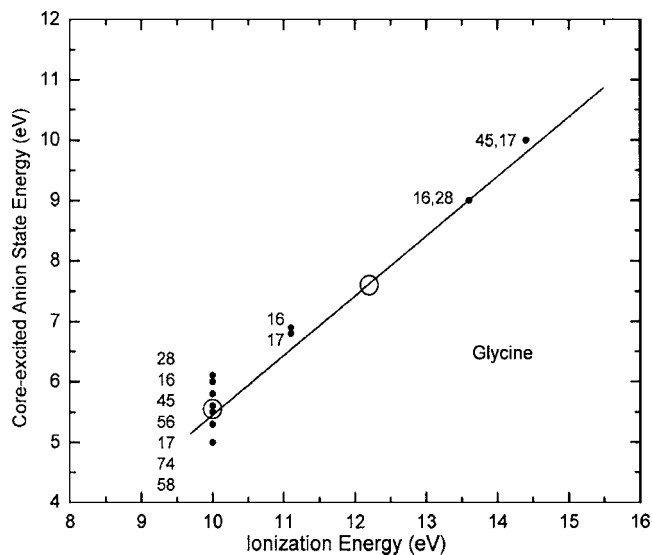


FIG. 4. The energies of the core-excited anion states of glycine, as represented by the peaks in the DEA yields, as a function of the ionization energies determined from PES. The open circles are the present data. The smaller filled circles are from Ref. 19.

2 is close to that between the first and third ionization energies (IEs) determined by photoelectron spectroscopy (PES).⁴⁵ We postulate therefore that the lower DEA peak arises from promotion out of the highest occupied molecular orbital (HOMO) and the upper from excitation out of HOMO-2. These two data points are shown as open circles in Fig. 4, which displays the energies of the core-excited anion states, as represented by the peaks in the DEA cross sections, as a function of the IEs. A line of unit slope is best fit to the two points to guide the eye. The peak energies of the various anion fragments observed by Ptasińska *et al.*¹⁹ are shown as closed circles. The number next to each point indicates the mass of the fragment in Da.

The energy range centered at 5.55 eV contains DEA peaks from a number of anion fragments. Some of these are quite small in relative magnitude, nevertheless, they fall within the full width at half maximum of the peak in the total DEA cross section, and we assume that they are associated with excitation out of the HOMO (IE=10.0 eV). The spread in peak energies could reflect differences in the energies of repulsive anion states that predissociate the initially formed anion state or possibly different thermodynamic thresholds for the fragments. Excitation out of the HOMO-1 (IE=11.1 eV) can be associated with peaks appearing in masses 16 and 17 lying at 6.8–6.9 eV, although these latter values are subject to error because of overlap with lower lying peaks. Continuing upward, DEA peaks in masses 16 and 28 appear in good agreement with excitation from the HOMO-3 (IE=13.7 eV), and similarly, contributions from masses 45 and 17 could be associated with the HOMO-4 (IE=14.4 eV). Similar correlations are found in alanine and proline (not shown), a result that is not surprising given their closely related structures.

The equation of the line in Fig. 4 is given by $\text{CES} = \text{IE} - 4.53$ (eV). The binding energy of these core-excited anion states relative to the ionization energies is consistent with the

assignment of the outer two electrons to a Rydberg-like ($3s$)² configuration. Such resonances have been previously observed in atoms and a number of small molecules. Their role in the DEA process in molecules containing hydroxyl and amino groups is discussed by Skalicky and Allan.⁴⁶ This paper provides a useful entry to the earlier literature as well. In contrast to the results of these authors who found only weak or no evidence for such resonances in the few unsaturated compounds they studied (phenol, pyrrole, and N, N-dimethylaniline), glycine appears to display them rather well. In part, this could be a result of the absence of data on H⁻ in their studies.

Clearly, a detailed assignment of these and other possible core-excited resonance states and their binding energies presents a considerable challenge to theory.

VI. CONCLUDING COMMENTS

Measurements of the yield of H⁻ in all the amino acids would be very useful as this appears to be the dominant component of DEA in the core-excited region. Measurements with higher signal to noise ratios in other fragments would also aid in the assignments of the core-excited resonances and lead eventually to a better understanding of the fragmentation processes. Observation of the peaks in the total DEA cross section that lie above the ionization energy should be possible in a modified version of our apparatus, and this work is planned. Finally, normalization to calculated ionization cross sections as carried out here can give more accurate values than available previously, but experiments in which the absolute target density is determined should be the long term goal.

ACKNOWLEDGMENTS

This work was supported in part by funding from the Nebraska Interdisciplinary Science Symposium. One of the authors (P.D.B.) thanks Professor S.J. Buckman and the Centre for Antimatter-Matter Studies at the Australian National University for their hospitality while portions of these data were analyzed. Another author (P.M.) kindly acknowledges the TASK Academic Computer Centre for the Computational Grant.

¹K. Aflatooni, A. M. Scheer, and P. D. Burrow, *J. Chem. Phys.* **125**, 054301 (2006).

²W. Hwang, Y. K. Kim, and M. E. Rudd, *J. Chem. Phys.* **104**, 2956 (1996).

³H. Deutsch, K. Becker, S. Matt, and T. D. Märk, *Int. J. Mass. Spectrom.* **197**, 37 (2000).

⁴S. Feil, K. Gluch, S. Matt-Leubne, P. Scheier, J. Limtrakul, M. Probst, H. Deutsch, R. Becker, A. Stamatovic, and T. D. Märk, *J. Phys. B* **37**, 3013 (2004).

⁵P. Mozejko and L. Sanche, *Radiat. Phys. Chem.* **73**, 77 (2005).

⁶Y. K. Kim and M. E. Rudd, *Phys. Rev. A* **50**, 3954 (1994).

⁷W. Hwang, Y. K. Kim, and M. E. Rudd, *J. Chem. Phys.* **104**, 2956 (1996).

⁸N. F. Mott, *Proc. R. Soc. London, Ser. A* **126**, 259 (1930).

⁹H. Bethe, *Z. Physik* **76**, 293 (1932).

¹⁰Y. K. Kim, W. Hwang, N. M. Weinberger, M. A. Ali, and M. E. Rudd, *J. Chem. Phys.* **106**, 1026 (1997).

¹¹M. A. Ali, Y. K. Kim, W. Hwang, N. M. Weinberger, and M. E. Rudd, *J. Chem. Phys.* **106**, 9602 (1997).

¹²M. J. Frisch, G. W. Trucks, H. B. Schlegel *et al.*, GAUSSIAN 03, Revision B.05, Gaussian, Inc., Pittsburgh, 2003.

¹³V. G. Zakrzewski and W. von Niessen, *J. Comput. Chem.* **14**, 13 (1994).

¹⁴L. Sanche and G. J. Schulz, *Phys. Rev. A* **5**, 1672 (1972).

¹⁵K. Aflatooni, B. Hitt, G. A. Gallup, and P. D. Burrow, *J. Chem. Phys.* **115**, 6489 (2001).

¹⁶M. Tronc, M. Allan, and F. Edard, *Proceedings of the ICPEAC 1987*, p. 335.

¹⁷M. V. Muftakov, Y. V. Vasil'ev, and V. A. Mazunov, *Rapid Commun. Mass Spectrom.* **13**, 1104 (1999).

¹⁸S. Gohlke, A. Rosa, E. Illenberger, F. Brüning, and M. A. Huels, *J. Chem. Phys.* **116**, 10164 (2002).

¹⁹S. Ptasinska, S. Denifl, A. Abedi, P. Scheier, and T. D. Märk, *Anal. Bioanal. Chem.* **377**, 1115 (2003).

²⁰S. Ptasinska, S. Denifl, P. Candori, S. Matejcik, P. Scheier, and T. D. Märk, *Chem. Phys. Lett.* **403**, 107 (2005).

²¹H. Abdoul-Carime and E. Illenberger, *Chem. Phys. Lett.* **397**, 309 (2004).

²²H. Abdoul-Carime, S. Gohlke, and E. Illenberger, *Chem. Phys. Lett.* **402**, 497 (2005).

²³A. Pelc, W. Sailer, P. Scheier, N. J. Mason, and T. D. Märk, *Eur. Phys. J. D* **20**, 441 (2002).

²⁴A. Pelc, W. Sailer, P. Scheier, M. Probst, N. J. Mason, E. Illenberger, and T. D. Märk, *Chem. Phys. Lett.* **361**, 277 (2002).

²⁵A. Pelc, W. Sailer, P. Scheier, N. J. Mason, E. Illenberger, and T. D. Märk, *Vacuum* **70**, 429 (2003).

²⁶V. S. Prabhudesai, D. Nandi, A. H. Kelkar, R. Parajuli, and E. Krishnakumar, *Chem. Phys. Lett.* **405**, 172 (2005).

²⁷I. Martin, T. Skalicky, J. Langer, H. Abdoul-Carime, G. Karwasz, E. Illenberger, M. Stano, and S. Matejcik, *Phys. Chem. Chem. Phys.* **7**, 2212 (2005).

²⁸T. N. Rescigno, C. S. Trevisan, and A. E. Orel, *Phys. Rev. Lett.* **96**, 213201 (2006).

²⁹See, for example, K. Aflatooni and P. D. Burrow, *J. Chem. Phys.* **113**, 1455 (2000).

³⁰M. F. Schmidt, K. K. Baldrige, J. A. Boatz *et al.*, *J. Comput. Chem.* **14**, 1347 (1993).

³¹See, for example, D. Chen and G. A. Gallup, *J. Chem. Phys.* **93**, 8893 (1990); S. W. Staley and J. T. Strnad, *J. Phys. Chem.* **98**, 116 (1994).

³²K. Aflatooni, G. A. Gallup, and P. D. Burrow, *J. Phys. Chem. A* **102**, 6205 (1998).

³³K. Aflatooni, G. A. Gallup, and P. D. Burrow, *J. Phys. Chem. A* **104**, 7359 (2000).

³⁴G. A. Gallup (unpublished).

³⁵R. K. Nesbit, *Phys. Rev. A* **24**, 1184 (1981).

³⁶A. U. Hazi, in *Molecular Resonance Phenomena*, edited by T. Rescigno, V. McKoy, and B. Schneider (Plenum, New York, 1978).

³⁷A. U. Hazi, *J. Phys. B* **11**, L259 (1978).

³⁸M. Allan, *J. Phys. B* **39**, 2939 (2006).

³⁹E. G. Diken, N. I. Hammer, and M. A. Johnston, *J. Chem. Phys.* **120**, 9899 (2004).

⁴⁰M. Gutowski, P. Skurski, and J. Simons, *J. Am. Chem. Soc.* **122**, 10159 (2000).

⁴¹H. Hotop, M.-W. Ruf, M. Allan, and I. I. Fabrikant, *Adv. At., Mol., Opt. Phys.* **49**, 85 (2003).

⁴²A. M. Scheer, K. Aflatooni, G. A. Gallup, and P. D. Burrow, *Phys. Rev. Lett.* **92**, 068102 (2004).

⁴³P. D. Burrow, G. A. Gallup, A. M. Scheer, S. Denifl, S. Ptasinska, T. Märk, and P. Scheier, *J. Chem. Phys.* **124**, 124310 (2006).

⁴⁴Y. V. Vasil'ev, B. J. Figard, V. G. Voinov, D. F. Barofsky, and M. L. Deinzer, *J. Am. Chem. Soc.* **128**, 5506 (2006).

⁴⁵P. H. Cannington and N. S. Ham, *J. Electron Spectrosc. Relat. Phenom.* **32**, 139 (1983).

⁴⁶T. Skalicky and M. Allan, *J. Phys. B* **37**, 4849 (2004), and references therein.

